TADAS LISAUSKAS

# RESEARCH OF CFRP STRENGTHENED FLEXURAL REINFORCED CONCRETE BEAMS

SUMMARY OF DOCTORAL DISSERTATION

TECHNOLOGICAL SCIENCES, CIVIL ENGINEERING (T 002)

Kaunas
2021

KAUNAS UNIVERSITY OF TECHNOLOGY

TADAS LISAUSKAS

# RESEARCH OF CFRP STRENGTHENED FLEXURAL REINFORCED CONCRETE BEAMS

Summary of Doctoral Dissertation
Technological Sciences, Civil Engineering (T 002)

2021, Kaunas

This doctoral dissertation was prepared at Kaunas University of Technology, Faculty of Civil Engineering and Architecture, Department of Civil Engineering and Architecture Competence Centre during the period of 2016–2020.

**Scientific Supervisor:**
Assoc. Prof. Dr. Mindaugas AUGONIS (Kaunas University of Technology, Technological Sciences, Civil Engineering, T 002)

**Scientific Advisor:**
Dr. Mario Rui Tiago ARRUDA (CERIS at University of Lisbon, Portugal, Technological Sciences, Civil Engineering, T 002)

**English Language Editor:** Armandas Rumšas (Publishing Office "Technologija")
**Lithuanian Language Editor:** Prof. dr. Gabija Bankauskaitė (Vilnius University)

**Dissertation Defence Board of Civil Engineering Science Field:**
Prof. Dr. Raimondas BLIŪDŽIUS (Kaunas University of Technology, Technological Sciences, Civil Engineering – T 002) – **chairman**;
Prof. Dr. Eglė JOTAUTIENĖ (Vytautas Magnus University, Technological Sciences, Mechanical Engineering – T 009);
Assoc. Prof. Dr. Peter KOTEŠ (University of Žilina, Technological Sciences, Civil Engineering – T 002);
Prof. Dr. Žymantas RUDŽIONIS (Kaunas University of Technology, Technological Sciences, Civil Engineering – T 002);
Assoc. Prof. Dr. Darius ZABULIONIS (Vilnius Gediminas Technical University, Civil Engineering – T 002).

The official defence of the dissertation will be held at 10:00 a.m. on the 27th of April 2021 at the public meeting of the Dissertation Defence Board of Civil Engineering Science Field in the Dissertation Defence Hall at Kaunas University of Technology.

Address: Donelaičio 73-403, LT-44249, Kaunas, Lithuania.
Phone. (+370) 37 300 042, fax (+370) 37 324 144, email doktorantura@ktu.lt

The summary of this doctoral dissertation was sent out on 26 March, 2021.
The doctoral dissertation is available on the internet at http://ktu.edu and at the library of Kaunas University of Technology (Donelaičio 20, LT-44239, Kaunas, Lithuania).

KAUNO TECHNOLOGIJOS UNIVERSITETAS

TADAS LISAUSKAS

# LENKIAMŲ GELŽBETONINIŲ SIJŲ, SUSTIPRINTŲ ANGLIES PLAUŠU, TYRIMAI

Daktaro disertacijos santrauka
Technologijos mokslai, statybos inžinerija (T 002)

2021, Kaunas

Disertacija rengta 2016–2020 metais Kauno technologijos universiteto Statybos ir architektūros fakultete, statybos ir architektūros kompetencijų centre.

**Mokslinis vadovas:**
Doc. dr. Mindaugas AUGONIS (Kauno technologijos universitetas, Technologijos mokslai, Statybos inžinerija, T 002)

**Mokslinis konsultantas:**
Dr. Mario Rui Tiago ARRUDA (CERIS, Aukštasis technikos institutas, Lisabonos universitetas, Portugalija, Technologijos mokslai, Statybos inžinerija, T 002)

**Anglų kalbos redaktorius:** Armandas Rumšas (Leidykla „Technologija“)
**Lietuvių kalbos redaktorius:** prof. dr. Gabija Bankauskaitė (Vilniaus universitetas)

**Statybos inžinerijos mokslo krypties disertacijos gynimo taryba:**
Prof. dr. Raimondas BLIŪDŽIUS (Kauno technologijos universitetas, technologijos mokslai, statybos inžinerija – T 002) – **pirmininkas**;
Prof. dr. Eglė JOTAUTIENĖ (Vytauto Didžioji universitetas, technologijos mokslai, mechanikos inžinerija – T 009);
Doc. dr. Peter KOTEŠ (Žilinos universitetas, technologijos mokslai, statybos inžinerija – T 002);
Prof. dr. Žymantas RUDŽIONIS (Kauno technologijos universitetas, technologijos mokslai, statybos inžinerija – T 002);
Doc. dr. Darius ZABULIONIS (Vilniaus Gedimino technikos universitetas, technologijos mokslai, statybos inžinerija – T 002).

Disertacija bus ginama viešame Statybos inžinerijos mokslo krypties disertacijos gynimo tarybos posėdyje 2021 m. balandžio 27 d. 10.00 val. Kauno technologijos universiteto Disertacijų gynimo salėje.

Adresas: K. Donelaičio g. 73-403, 44249 Kaunas, Lietuva.
Tel. + 370 37 300 042; faks. + 370 37 324 144; el. paštas doktorantura@ktu.lt

Disertacijos santrauka išsiųsta 2021 m. kovo 26 d.
Su daktaro disertacija galima susipažinti interneto svetainėje http://ktu.edu ir Kauno technologijos universiteto bibliotekoje (K. Donelaičio g. 20, 44239 Kaunas).

# INTRODUCTION

## Relevance of the scientific problem

Strengthening of reinforced concrete structures is highly relevant since the moment of the emergence of reinforced concrete. The reasons for strengthening can be various, but the main ones are the insufficient strength and/or stiffness. It is especially relevant when there is necessity to increase the load-bearing capacity due to additional loads. Due to its properties, carbon fibre (CFRP) is a suitable material for increasing the load-bearing capacity of reinforced concrete structures. The tensile strength of carbon fibre can be greater than 2000 MPa. What is more, using this kind of a thin material for strengthening does not increase the cross-section of the structure. Furthermore, the preparation for strengthening is relatively easy, and this kind of strengthening increases corrosion resistance. Despite the relatively high cost, carbon fibre is used to strengthen beams, columns, slabs, and bridge structures.

It is common that, in most cases, already existing structures are cracked. Thus, it is difficult to evaluate whether the strengthened structure would withstand the design loads. Therefore, analysis of flexural cracked and carbon fibre strengthened reinforced concrete beams has been carried out in this dissertation. An analytical method evaluating the bond (shear) force of the cracked (with low cracking intensity) element and tangential (shear) stress between the carbon fibre and the concrete over the length of the element has been proposed.

## The aim of the dissertation

The aim of this dissertation is to propose an alternative analytical methodology that would allow to calculate the bond (shear) force and tangential (shear) stress between the carbon fibre and the concrete of the uncracked and cracked (with low cracking intensity) flexural element while estimating the slip of the layers over the length of the element.

## The objectives of the dissertation

1. To carry out a review of the state-of-the-art research of the flexural reinforced concrete beams strengthened with carbon fibre. To review the methods of strengthening of reinforced concrete beams and the properties of fibre. To analyse the analytical methods describing the strength and stiffness of reinforced concrete beams strengthened with CFRP.
2. To perform experimental investigation of the stiffness and strength of flexural cracked reinforced concrete beams strengthened with CFRP and to measure the parameters necessary to determine the slip of the contact zone between concrete and CFRP.

3. To propose an analytical methodology that estimates and describes the bond (shear) force and tangential (shear) stress between the carbon fibre and the concrete in the cracked flexural composite while estimating the slip of the layers over the length of the element. To calculate the characteristics of the composite beam while using the methods proposed by other authors or the general calculation principles. The analytical results are then compared with the experimental results.
4. To perform calculations of the flexural reinforced concrete beams strengthened with CFRP by using the finite element method.

**Research methodology**

1. Analysis of the scientific publications, books and standard *Euronorms*.
2. Composite beams are tested with the universal press. Cracks are measured with a binocular gauge, a crack ruler, and dial gauges. Concrete deformations are measured by using dial gauges. The slip of the contact area between the carbon fibre and the concrete in the composite beam is obtained by measuring the deformations while using strain gauges. Deflections are measured by using linear displacement sensors.
3. Calculation was performed by the iteration method, the theory of the built-up bars, ACI, ISIS, *fib*, EC2 and other methods.
4. Numerical calculations were performed by using the finite element software *Abaqus*.

**Scientific novelty**

An analytical model of the shear force and stress between the carbon fibre and the concrete of a flexural uncracked and cracked (with low cracking intensity) composite was developed thus allowing estimation of the slip of the layers over the length of the element. This model calculates the significantly increased shear stress in the crack zone between carbon fibre and concrete leading to a faster loss of contact in this zone.

The influence of the scale of damage of reinforced concrete beams on the bearing capacity and stiffness of carbon fibre strengthened beams was investigated, and it was found that the bearing capacity of those beams with the largest initial crack width increased the most.

**The practical value of research findings**

An analytical method for determining the bond force of flexural cracked (with low cracking intensity) composites between two layers by estimating their slip has been proposed. The analytical model can estimate the bond stiffness of the layers under different load cases and can be applied to the design of strengthened structures. The proposed method not only makes it relatively easier to calculate the shear stress and shear forces between layers by avoiding the solution of differential equations compared to the theory of the built-up bars, but also estimates the significant effect of cracks. In this way, the proposed method can be used for estimating the contact behaviour of a composite when a crack opens; hence this method is denoted by a wider range of applications.

**Statement presented for the defence**

The shear stress of flexural reinforced concrete structures strengthened with carbon fibre in the tensile concrete zone after opening the crack can be predicted with sufficient accuracy by estimating the variable stiffness of the element cross-section in the fibre anchoring zone at the crack.

**Approval of work results**

4 scientific publications have been published on the topic of the dissertation: 1 article in the *Clarivate Analytics Web of Science* database publication with an impact factor, 1 article in publications of other international databases, 2 articles in international publications proceedings of international conferences.

# 1. LITERATURE REVIEW

## 1.1. Application of flexural reinforced concrete beams strengthened with carbon fibre and usual types of failure

There are two main ways of strengthening reinforced concrete structures: strengthening of new structures or strengthening of the already existing structures with the carbon fibre. The second case is common when the structure was used for some time, but it no longer satisfies the necessary requirements of the structure due to the existing or possible external actions in the future. Possible problems may be related to the strength of the normal or the diagonal cross-section, the excessive crack widths or deflections. To solve those issues, a suitable construction material is the carbon fibre as it possesses high strength, is corrosion resistant and is simple regarding strengthening. An example could be a comparison with a steel strip which could also be used to strengthen reinforced concrete structures, but the drawback is the fact that the steel strip is relatively rigid, heavy and difficult to glue to the surface. Another advantage of carbon fibre strengthened structures is that this kind of strengthening of the structure does not increase the width and height of structures, which helps saving the space of the rooms and maintaining the functionality of the structure.

There are a number of structures to which carbon fibre strengthening can be applied: strengthening of the tensile zone of reinforced concrete beams, slabs, columns, and bridge structures.

In order to understand the behaviour of strengthened structures, it is necessary to understand the usual types of failure of strengthened structures. In Figure 1, all possible types of failure of the reinforced concrete beam strengthened with carbon fibre are described by Esfahani et al., 2007. In Figure 1, we present: a) the type of failure when the weakest part of the composite beam is the compressive concrete, b) the rupture of the tensile fibre due to the insufficient tensile strength, c), d) debonding of the carbon fibre from the concrete due to the insufficient anchorage length, e, f) a type of failure when a developed normal or diagonal crack causes a loss of the bond between the carbon fibre and the concrete and debonding of the carbon fibre starts away from the ends of the carbon fibre strip. The developed crack and the loss of contact expands towards the ends of the carbon fibre strip until the structure fails. This type of failure may occur when the reinforcement bars are corroded, and the reinforcement ratio of the structure is high (the distance between the rebars is small). In Figure 1.1. g) the failure of the diagonal cross-section of the composite beam is shown.

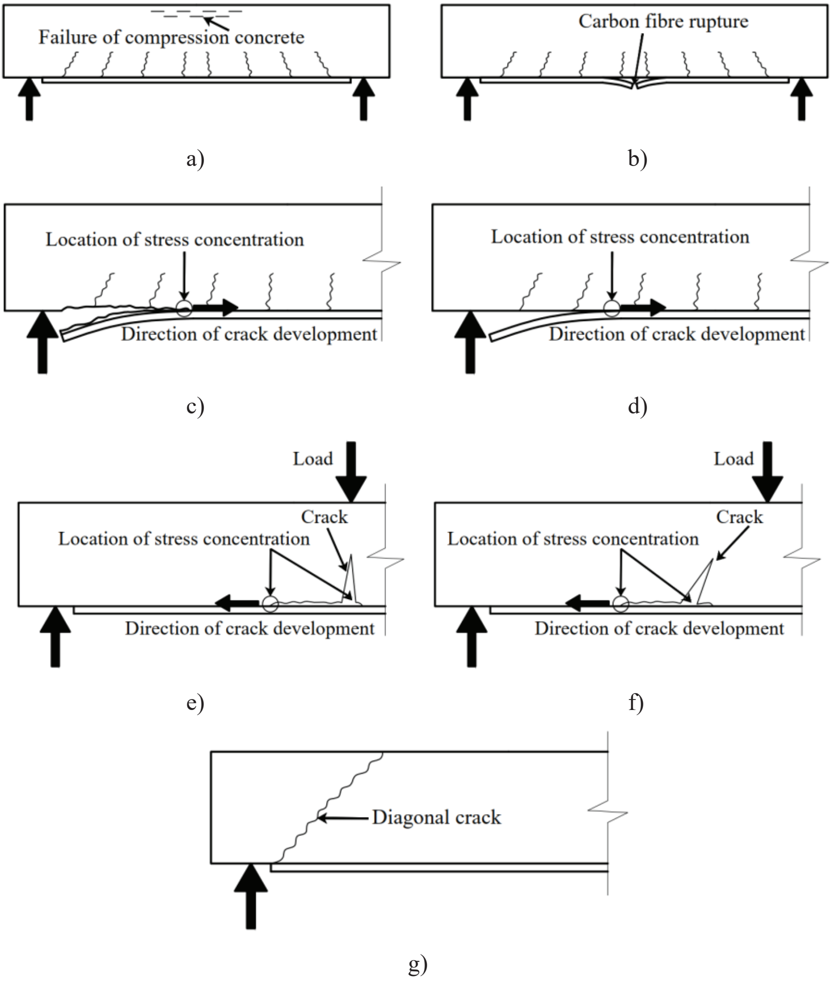


**Figure 1** Types of failure of reinforced concrete beams strengthened with carbon fibre: (a) due to the loss of the strength of concrete in the compression zone; (b) carbon fibre rupture; c, d) insufficient anchorage length; e, f) loss of the carbon fibre bond to concrete; (g) loss of the load-bearing capacity in the diagonal section

## 1.2. Behaviour of the contact zone between carbon fibre and concrete in composite structures

The contact zone between the carbon fibre and the concrete of reinforced concrete structures strengthened with the carbon fibre have been studied by a number of authors (Alhassan et al., 2020; Chen et al., 2018; *fib*, 2001; Lisauskas et al., 2018; Lorenzis et al., 2001). In this case, it is extremely important not only to obtain the maximum contact stress, but also their distribution over the length of the element.

The possible loss of the bond between the carbon fibre and the concrete is shown in Figure 1. c–f. The first two types of failure (cohesive failure in the concrete or debonding of the carbon fibre from the concrete) usually occur when there is a loss of the bond between the carbon fibre and the concrete. The tensile force in the carbon fibre is transferred to the concrete by tangential (shear) stress via the bond. When the maximum tangential stress (the bond strength limit) is reached, the loss of the bond starts with the aforementioned types of failure. During the loss of the bond, specific changes in the zone where the maximum tangential stress occur are observed (Guo, 2003; Guo et al., 2005). This means that only a part of the bond zone is effective. When cracks develop in concrete, the bond is lost at the cracking zone. However, the nearby zone is also activated at the same time (the tangential stress curve and the maximum value shifts to the support). This redistribution of tangential stress is clearly seen in Figure 2 when the maximum shear force between carbon fibre and concrete (0.999Pmax) is reached. As the shear force increases by 0.01% (0.9999Pmax), the tangential stress and their maximum value redistribute to the nearby zone. This means that the anchorage force cannot be increased by increasing the anchorage length, and the carbon fibre strength limit will never be reached regardless of how long the anchorage length is. Thus, there is always some specific effective anchorage length that is sufficient to achieve the maximum bond. From the mechanical point of view, this is explained by the bond stress-slip dependence curve (Elghazy et al., 2018; Mofrad et al., 2019; Mukhtar et al., 2018; Wan et al., 2018). This dependence is illustrated in Figure 3. It is noticeable that there is an initial shear stress increase as the slip between the carbon fibre and the concrete increases. When the maximum stress is reached, the stress starts to decrease, but the slip increases furthermore, and the force of adhesion does not decrease. It means that the maximum tangential stress occurs elsewhere.

Figure 2 shows the test setup and the results of single lap pullout bond test (Guo, 2003). The aim of the test is to investigate the distribution of the carbon fibre bond to concrete over the length of the element. According to those results, it is evident that from 0 to 50% of the failure load, the maximum tangential stress is obtained at the end of the element. As the load increases, the maximum stress is obtained further from the edge. Thus, the higher the load is, the further the maximum tangential stress is from the edge. It should be noted that the tangential stress does not exceed the maximum tangential stress obtained at 50% of the failure load. By analysing those curves, it can be concluded that once the maximum tangential stress at the end of the carbon fibre has been reached, a brittle bond failure occurs, and the stress redistributes to the nearby zone. There is no plastic distribution of the tangential stress so that it would stretch over the contact zone during the whole loading procedure.

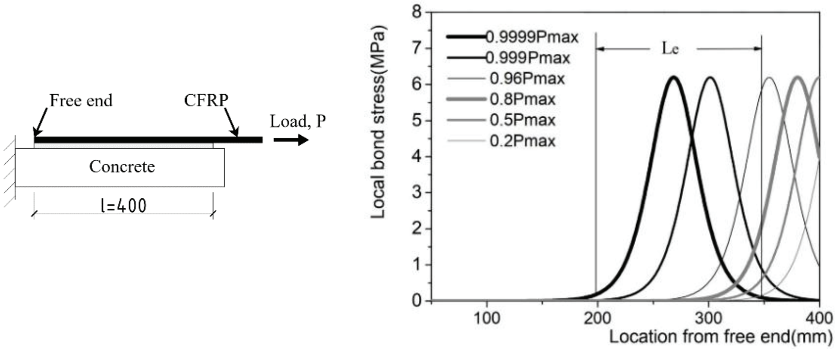


a) b)

**Figure 2** a) Sketch of the single lap pullout bond test; b) Bond stress along the length of the element under various loads (Guo, 2003)

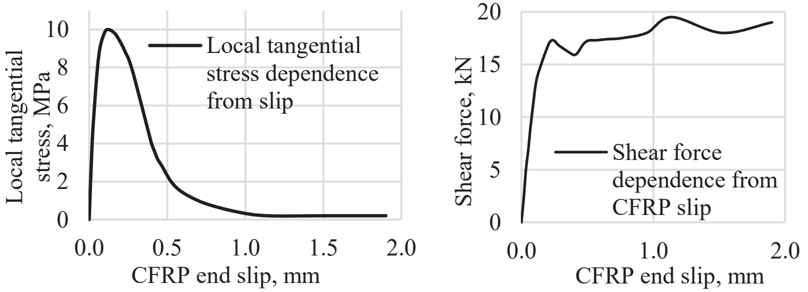


a) b)

**Figure 3** a) Local tangential stress dependence from the slip in the contact zone between carbon fibre and concrete; b) Shear force dependence from the CFRP end slip in the contact zone between carbon fibre and concrete (Wan et al., 2018)

## 2. EXPERIMENTAL RESEARCH OF REINFORCED CONCRETE BEAMS STRENGTHENED WITH CARBON FIBRE

### 2.1. Material properties and their statistical evaluation

The experiment was performed by testing nine reinforced concrete beams. Three reinforced concrete beams were formed during each casting using a different concrete composition. To determine the strength of the concrete, concrete cubes with the dimensions of ~ 100×100×100 were tested. The cubes were tested according to LST EN 12390-3:2009 (LST EN 12390-3:2009.

Sukietėjusio betono bandymai. 3 dalis. Bandinių gniuždomasis stipris, 2009). The test results for the concrete cubes are presented in Table 1.

The modulus of elasticity of the concrete was determined by tests carried out according to LST EN 12390-13:2013 (LST EN 12390-13:2013. Sukietėjusio betono bandymai. 13 dalis. Kirstinio tamprumo modulio nustatymas gniuždant, 2013). Prisms with the dimensions of ~ 300×100×100 mm were used for the tests. Table 1 shows the average strength, the mean modulus of elasticity, the confidence interval, and Student's coefficient for separate concrete cubes.

**Table 1** Average values of the compressive strength of concrete cubes, modulus of elasticity of the prisms, confidence interval with 95% reliability and Student's coefficient values

| Title | series 1 | series 2 | series 3 |
|---|---|---|---|
| Average compressive strength $f_{cm,cube}$, MPa | 57.0 | 61.4 | 53.0 |
| Confidence interval $X_{k95}$, MPa | (53.7; 60.3) | (55.6; 67.3) | (50.2; 55.8) |
| Student's coefficients, $t_{vd}$ | 1.782 | 1.725 | 1.746 |
| Average modulus of elasticity $E_{cm}$, GPa | 40.5 | 45.0 | 37.6 |
| Confidence interval $X_{k95}$, MPa | (37.3; 43.6) | (42.5; 47.6) | (35.4; 39.8) |
| Student's coefficients, $t_{vd}$ | 2.353 | 2.132 | 2.132 |

Reinforced concrete beams were reinforced by using B500B grade rebars. Rods with the diameter of Ø12 mm were selected as the longitudinal reinforcement. Ø 6 mm rods were used as the transverse reinforcement. During the tensile test, the actual yield strength of the reinforcement was obtained as $f_y$ = 600 MPa. The ultimate strength was obtained as $f_u$ = 708 MPa. The modulus of elasticity of the reinforcement was $E_s$ = 200 GPa (LST EN 1992-1-1. Eurokodas 2. Gelžbetoninių konstrukcijų projektavimas. 1-1 dalis, 2007).

The reinforced concrete beam is strengthened by using the carbon fibre. The carbon fibre bond to the concrete is ensured by epoxy resin. The material properties according to the values declared by the manufacturer (DRIZORO) were assumed. The ultimate strength of the carbon fibre was obtained as $f_{CFRP}$ =3 400 MPa, the limit relative deformations as $\varepsilon_{CFRP,u}$=0.015, the modulus of elasticity as $E_{CFRP}$=230 GPa, the thickness of the carbon fibre sheets as $t_{CFRP}$=0.167 mm, the ultimate strength of epoxy resin as $f_{Epox}$ =29 MPa, the modulus of elasticity as $E_{Epox}$=1.5 GPa, and the thickness of resin as $t_{Epox}$=0.727 mm.

## 2.2. Experimental program

Nine reinforced concrete beams were formed and later strengthened by using carbon fibre. The beams were cast in separate batches of three beams due to the limited number of formworks. To obtain cracked beams before strengthening with carbon fibre, hardened beams were loaded with an initial load. When a certain level of damage and load had been reached, the beam was unloaded. Table 2 presents the beam specimens by describing the level of the beam damage and the quantity of the carbon fibre. Three types of damage were observed. Series A beams had no initial cracks (no initial load), Series B beams had a 0.4 mm crack (at the 60 kN load), Series C beams were loaded until the reinforcement reached the yield strength (at the 95 kN load approximately).

**Table 2** Quantity of carbon fibre and damage of beams

| Type of beam | Number of carbon fibre layers, pcs. | The length of the carbon fibre $l$, m | Width of the initial crack $\omega_p$, mm |
|---|---|---|---|
| A1 | 1 | 0.7 | Without initial cracks |
| B1 | 1 | 0.7 | 0.4 mm |
| C1 | 1 | 0.7 | Rebar reached yield strength (0.9 mm) |
| A2 | 3 | 1.0 | Without initial cracks |
| B2 | 3 | 1.0 | 0.4 mm |
| C2 | 3 | 1.0 | Rebar reached yield strength (1.0 mm) |
| A3 | 1 | 1.0 | Without initial cracks |
| B3 | 1 | 1.0 | 0.4 mm |
| C3 | 1 | 1.0 | Rebar reached yield strength (1.1 mm) |

During the loading, three main normal cracks opened in the reinforced concrete beams. One crack was in the mid-length of the beam, the other two were in the projection of the load application point.

The failure of the reinforced concrete beam strengthened with the carbon fibre was assumed when the carbon fibre debonded. Two cases of carbon fibre debonding were observed. They are shown in Figure 4. The carbon fibre of the third series of the beams debonded together with the concrete, while the carbon fibre of the first and second series of the beams debonded with almost no damage to the concrete. From the results of the debonding, it can be stated that the weakest part of the contact zone between the carbon fibre and the concrete was the strength of the concrete (cohesion) for the third series of the beams and the bond between the carbon fibre and the concrete (adhesion) for the first and the second series beams.

a) b)

**Figure 4** View of the concrete after the debonding at the end of the carbon fibre: a) view of the third series beam; b) view of the first and second series beams

In Figure 5, the scheme of the four-point bending experiment of the composite beam is presented. A beam with the span of 1.2 m is tested. The height and width of the beam is 200 mm and 160 mm, respectively. The length of the pure bending zone is 250 mm. Hinges are used at the supports and at the load application point to prevent additional unexpected stress in the cross-section of the beam.

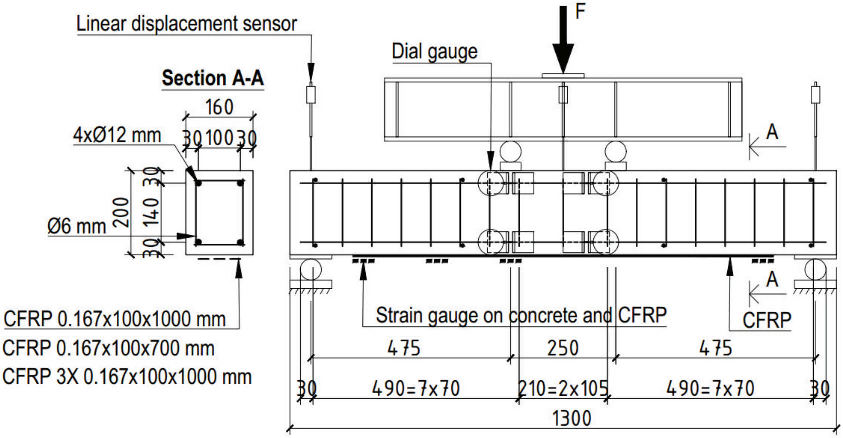


**Figure 5** Test setup and details of composite beams

## 2.3. Experimental studies of stiffness and strength of flexural reinforced concrete beams strengthened with carbon fibre

The failure forces and the mid-span deflections at the loading force of 100 kN are presented in Table 3. The failure force is assumed to be the load when the carbon fibre debonds from the R/C beam. The deflection $f$ is assumed without estimating the initial deflection, while the deflection $f_\Sigma$ is calculated by estimating the initial deflection. The initial deflection was obtained by loading and then unloading the R/C beam. The remaining deflection (the plastic beam deformation) is assumed as the residual deflection.

**Table 3** Failure force of the composite beam and deflection of the span under the load of 100 kN

| Beam | Failure force $F$, kN | Deflection $f$, mm | Deflection by estimating the initial residual deflection $f_\Sigma$, mm |
|---|---|---|---|
| A1 | 110.2 | 3.65 | 3.65 |
| B1 | 116.2 | 3.11 | 4.14 |
| C1 | 117.6 | 3.39 | 4.91 |

| Beam | Failure force $F$, kN | Deflection $f$, mm | Deflection by estimating the initial residual deflection $f_{\Sigma}$, mm |
|---|---|---|---|
| A2 | 103.7 | 2.98 | 2.98 |
| B2 | 127.3 | 2.48 | 2.88 |
| C2 | 138.2 | 2.88 | 5.88 |
| A3 | 120.9 | 4.12 | 4.12 |
| B3 | 124.1 | 3.23 | 3.65 |
| C3 | 133.0 | 3.43 | 6.55 |

The maximum load-bearing capacity was obtained for C-series composite beams which had the largest initial cracks. The lowest load-bearing capacity was obtained for the uncracked beams. The concrete of the B and C series composite beams reached elastic-plastic deformations after unloading the R/C beam (Daugevičius, 2010); therefore, steel reinforcement had initial deformations (stress). The series B and C beams which were strengthened with carbon fibre had the same amount of relative deformations in the carbon fibre but higher reinforcement relative deformations compared to the series A beams. The higher relative deformations in the reinforcement of the series B and C beams result in a higher bearing capacity compared to the series A beams.

Another reason for the higher load-bearing capacity of the B and C series beams is the curvature. A larger curvature (deflection) results in a higher debonding force of the carbon fibre which is perpendicular to the surface of the contact zone between the carbon fibre and the concrete. The load-deflection curves are presented in Figure 6.

a)

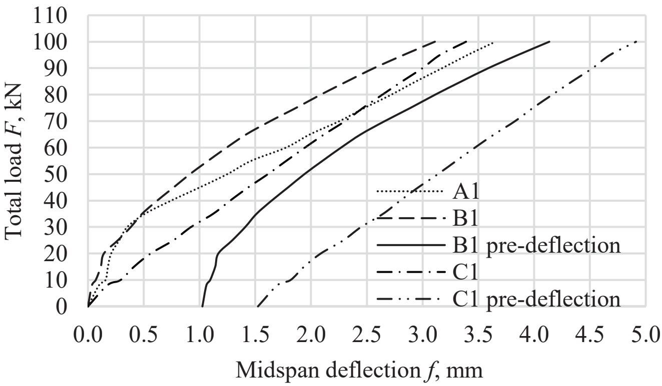

b)

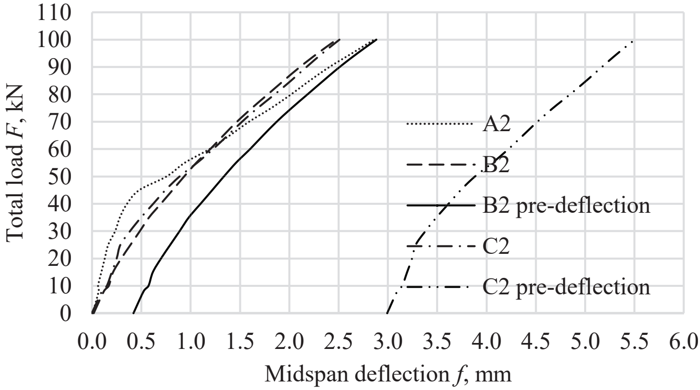


c)

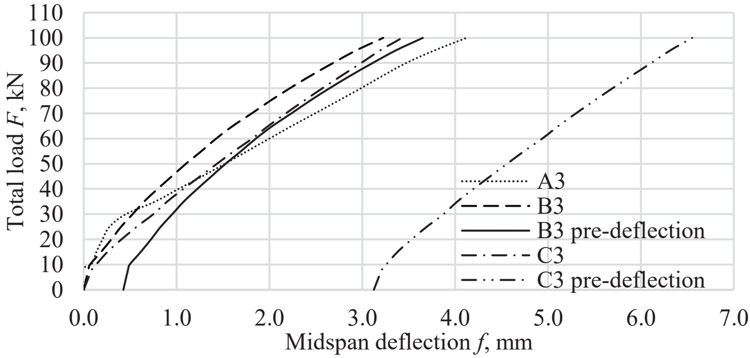


**Figure 6** Load-deflection curves: a) series 1 beams; b) series 2 beams; c) series 3 beams

## 3. ANALYTICAL RESEARCH OF REINFORCED CONCRETE BEAMS STRENGTHENED WITH CARBON FIBRE

### 3.1. Analytical model for estimating the influence of the layer bond for stiffness of layered structures

When calculating reinforced concrete structures strengthened with carbon fibre, we use the universal iteration method (Zadlauskas, 2013). The advantage of this method is that the physically nonlinear stress-strain dependency curve of the concrete can be evaluated. Composite beams were calculated by using the iteration method, the results of which are presented in Subsection 4.2.

The basis of the elastic body iteration method is Hooke's law. When plastic deformations of the material occur, the relative deformations of the cross-section are obtained by applying the deformation modulus. The general analytical expression of the iteration method is shown in Equation 3.1. The calculation via the iteration method is started by dividing the cross-section of an element into the separate layers. Each layer has its own stiffness. The expression of the stiffness matrix is shown in Equation 3.2. The physical nonlinearity of the concrete is evaluated via the modulus of deformation. The slip between the layers can be estimated by introducing the coefficient $k_{sukib}$. When $k_{sukib.}$=1, the bond is perfect. When $k_{sukib.}$=0 – there is no bond, and the carbon fibre can slip. The calculation scheme of the cross-section, the relative deformations and stress distribution schemes are presented in Figure 7.

$$[E_{stand}]\{\boldsymbol{\varepsilon}\} = \{\mathbf{F}\} \tag{3.1}$$

where $[E_{stand}]$ is the stiffness matrix (3.2); $\{\boldsymbol{\varepsilon}\}$ is the vector of the relative deformations (3.3); $\{\mathbf{F}\}$ is the vector of the loads (3.4)

$$[E_{stand}] = \\ = \begin{bmatrix} 1 & -2 & 1 & 0 & \cdots & 0 \\ 0 & 1 & -2 & 1 & \cdots & 0 \\ 0 & 0 & 1 & -2 & \cdots & 0 \\ 0 & 0 & 0 & 1 & \cdots & 1 \\ E_1A_1 & E_2A_2 & E_3A_3 & E_4A_4 & \cdots & k_{sukib.}E_nA_n \\ 0 & E_2A_2h_i & 2E_3A_3h_i & 3E_4A_4h_i & \cdots & k_{sukib.}(1-n)E_nA_nh_i \end{bmatrix} \tag{3.2}$$

where $E_i$ is the modulus of deformation of the i-th layer; $A_i$ is the the cross-sectional area of the i-th layer

$$\{\boldsymbol{\varepsilon}\} = \{\boldsymbol{\varepsilon_1} \quad \boldsymbol{\varepsilon_2} \quad \boldsymbol{\varepsilon_3} \quad \boldsymbol{\varepsilon_4} \quad \cdots \quad \boldsymbol{\varepsilon_n}\}^T \tag{3.3}$$

where $\boldsymbol{\varepsilon}_i$ is the relative deformations of the i-th layer

$$\{\mathbf{F}\} = \{\mathbf{0} \quad \mathbf{0} \quad \mathbf{0} \quad \mathbf{0} \quad \cdots \quad \mathbf{M}\}^T \tag{3.4}$$

where **M** is the bending moment

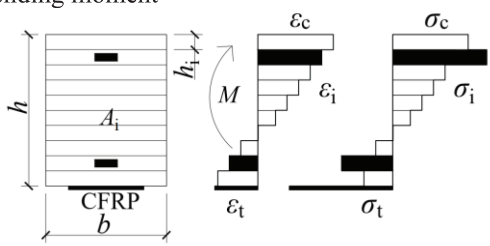


**Figure 7** Calculation scheme of the cross-section of the iteration method, relative deformations, and stress distribution schemes

## 3.2. Formation of the analytical model for estimating the distribution of the shear force and tangential stress in a two-layer contact zone over the length of the element

A calculation methodology describing the bond (shear) force and the tangential stress between the concrete and the carbon fibre is developed. In Figure 8, the calculation scheme of the two-layer element and the distribution of the relative deformations of the layers from the internal forces are presented. $M_{Ek}$ (Equation 3.5) is the external impact acting on the element, $M_1$ and $M_2$ are the bending moments acting on the first and second layer from the external moment distributed according to the bending stiffness. In Figure 8, the first layer is the reinforced concrete beam, the second layer is the carbon fibre.

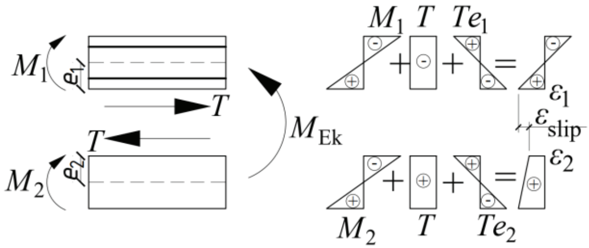


a) b)

**Figure 8** a) Calculation scheme of the two-layer element; b) Schemes of distribution of the relative deformations from the internal forces

$$M_{\mathrm{Ek}} = M_1 + M_2 \tag{3.5}$$

The composite beam is loaded with external impact, and the curvature of beam two layers is the same (3.6):

$$\frac{1}{r_1} = \frac{1}{r_2} \tag{3.6}$$

The bending moments (3.7) are inserted from the curvature Equation (3.6). The bending moment is calculated with regard to the centroid of each element:

$$\frac{M_1 - T \cdot e_1}{E_{\mathrm{c}} \cdot I_1} = \frac{M_2 - T \cdot e_2}{E_{\mathrm{CFRP}} \cdot I_{\mathrm{CFRP}}} \tag{3.7}$$

where: $T$ is the bond (shear) force; $E_{c,CFRP}$ is the modulus of elasticity of the concrete and carbon fibre, respectively.

As a simplification, when deriving the formulas, the ratios of the stiffness of the first and second layers are marked by using the symbol α (3.8):

$$\alpha = \frac{E_c \cdot I_1}{E_{CFRP} \cdot I_{CFRP}} \tag{3.8}$$

Figure 8 b) shows the relative deformations of the cross section layers from the internal forces and the slip between the first and the second layers. According to this figure, the Equation of slip (3.9) is derived:

$$\varepsilon_{slip} = \varepsilon_1 - \varepsilon_2 \tag{3.9}$$

According to the scheme in Figure 8 b), the relative deformations of the first (3.10) and the second (3.11) layers are expressed:

$$\varepsilon_1 = \frac{M_1}{W_1 \cdot E_c} - \frac{T}{A_c \cdot E_c} - \frac{T \cdot e_1}{W_1 \cdot E_c} \tag{3.10}$$

$$\varepsilon_2 = -\frac{M_2}{W_2 \cdot E_{CFRP}} + \frac{T}{A_{CFRP} \cdot E_{CFRP}} + \frac{T \cdot e_2}{W_2 \cdot E_{CFRP}} \tag{3.11}$$

where: $W_{1,2}$ is the section modulus of the first and second layers, respectively; $A_{c,CFRP}$ is the area of the cross section of the concrete and carbon fibre, respectively.
Equations 3.10 and 3.11 are then inserted into Expression 3.9 and rearranged. The bond (shear) force of the carbon fibre over the cross-sectional length (3.12) is obtained then:

$$T(x) = \left( \varepsilon_{slip}(x) - \frac{M_{Ek}(x)}{W_1 \cdot E_c \cdot \left(1 + \frac{1}{\alpha}\right)} - \frac{M_{Ek}(x)}{W_2 \cdot E_{CFRP} \cdot (1 + \alpha)} \right) / \left( \frac{\frac{e_1}{\alpha} - e_2}{W_1 \cdot E_c \cdot \left(1 + \frac{1}{\alpha}\right)} - \frac{1}{A_c \cdot E_c} - \frac{e_1}{W_1 \cdot E_c} + \frac{e_2 \cdot \alpha - e_1}{W_2 \cdot E_{CFRP} \cdot (1 + \alpha)} - \frac{1}{A_{CFRP} \cdot E_{CFRP}} - \frac{e_2}{W_2 \cdot E_{CFRP}} \right) \tag{3.12}$$

According to the selected calculation scheme and after replacing the concentrated forces with the distributed load (Figure 9), Equation (3.13) for the slip of the cross-sectional layers varying along the element length $\varepsilon^*_{slip}(x)$ is expressed. The multiplier before the coefficient $k$ describes the maximum possible slip between the layers over the length of the element depending on the value of the bending moment.

$$\varepsilon_{\text{slip}}(x) = k \cdot \left(\frac{M_1(x)}{W_1 \cdot E_{\text{c}}} + \frac{M_2(x)}{W_2 \cdot E_{\text{CFRP}}}\right) \tag{3.13}$$

where: $k$ is the coefficient estimating slippage (varies from 0 to 1.0; when $k$=0, there is maximum slippage, when $k$=1, there is no slippage).

The bending scheme of a simple-span composite beam is presented in Figure 9.

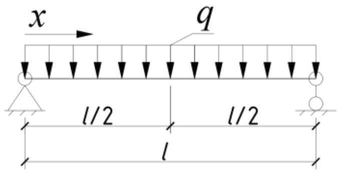


**Figure 9** Bending scheme of a simple-span composite beam

The tangential contact stress is obtained by differentiating the contact (shear) force along the axis of the element (Balevičius at al., 2018; Zabulionis, 2005; Ржаницын, 1982):

$$\tau(x) = \frac{\partial T(x)}{b_{\text{CFRP}} \cdot \partial x} \tag{3.14}$$

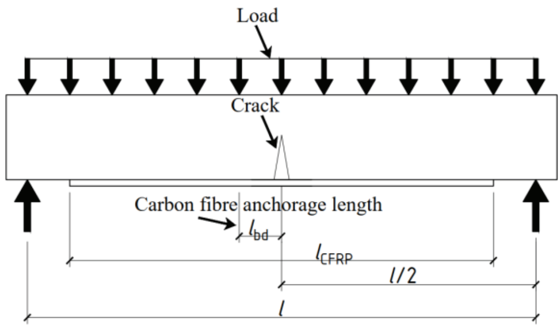


**Figure 10** Calculation scheme of the bond (shear) force between the carbon fibre and the concrete of the cracked reinforced concrete beam strengthened with carbon fibre

The proposed method of the analytical research will be applied for cracked reinforced concrete structures strengthened with carbon fibre. Calculations will be carried out for a composite beam having a crack in the middle of the span. The general view of the beam and the calculation scheme is presented in Figure 10. When fibre is bonded only to the middle part of the beam and not to its entire length, the slip is calculated according to the corrected Equation 3.13. To take this factor into account, the equation for calculating the slip is modified:

$$\varepsilon_{\text{slip}}^{*}(x) = k \cdot \left(\frac{M_1(x)}{W_1 \cdot E_{\text{c}}} + \frac{M_2(x)}{W_2 \cdot E_{\text{CFRP}}}\right) + (1-k) \cdot \left(\frac{M_1\left(\frac{l - l_{\text{CFRP}}}{2}\right)}{W_1 \cdot E_{\text{c}}} + \frac{M_2\left(\frac{l - l_{\text{CFRP}}}{2}\right)}{W_2 \cdot E_{\text{CFRP}}}\right) \quad (3.15)$$

where: $l_{\text{CFRP}}$ is the length of the carbon fibre

At the crack location, there is no bond between the carbon fibre and the concrete, and thus the slip at the crack location is the maximum possible. Further from the crack, the bond between the carbon fibre and the concrete starts to increase until it reaches a value equal to that of the composite beam without the cracks. This distance at which the carbon fibre is fully anchored is marked as $l_{\text{bd}}$. The slip of the cross-section layers in the crack action zone varying along the length of the element is expressed in Equation 3.16:

$$\varepsilon_{\text{slip,lbd}}^{*}(x) = k_{\text{lbd}}(x) \cdot \left(\frac{M_{1,\text{lbd}}(x)}{W_1 \cdot E_{\text{c,lbd}}(x)} + \frac{M_{2,\text{lbd}}(x)}{W_2 \cdot E_{\text{CFRP}}}\right) + \left(1 - k_{\text{lbd}}(x)\right) \cdot \left(\frac{M_1\left(\frac{l - l_{\text{CFRP}}}{2}\right)}{W_1 \cdot E_{\text{c}}} + \frac{M_2\left(\frac{l - l_{\text{CFRP}}}{2}\right)}{W_2 \cdot E_{\text{CFRP}}}\right) \quad (3.16)$$

where: $k_{\text{lbd}}(x)$ is the coefficient estimating the slippage in the crack influence zone over the length of the element expressed by the linear function (3.17); $M_{1,\text{lbd}}(x)$, $M_{2,\text{lbd}}(x)$ is the bending moment of the first and second layer (element), respectively, caused by the external moment in the crack influence zone, varying along the length of the element; $E_{\text{c,lbd}}(x)$ is the modulus of deformation of the concrete in the crack influence zone, varying along the length of the element expressed by the exponential Function (3.18)

The coefficient estimating the slip in the zone of influence of the crack over the length of the element is expressed by the linear function as follows:

$$k_{\text{lbd}}(x) = k + (1-k)\frac{(x - \frac{l}{2} + l_{\text{bd}})}{l_{\text{bd}}} \quad (3.17)$$

where: $l_{\text{bd}}$ is the distance required for carbon fibre to fully anchor.

The variation of the concrete deformation modulus in the crack influence zone can be described by the linear function, but a certain jump in the shear stress curve is obtained. To avoid a jump between the shear stress in the zone of influence of the crack and the non-cracked part, the exponential function is used.

The power of this function depends on the stiffness ratio of the layers and the bonding length of the carbon fibre but does not affect the maximum stress.

$$E_{\mathrm{c,lbd}}(x) = a \cdot x^{v} + c \tag{3.18}$$

where: $a$ is the incremental function multiplier (3.19); $v$ is the power indicator (obtained by approximation on a case-by-case basis; series 1 – 12.55; series 2 – 1.88; series 3 – 2.67); $c$ is the incremental function Constant (3.20).

Incremental function multiplier:

$$a = \frac{E_{\mathrm{c,cr}} - E_{\mathrm{c}}}{\left(\frac{l}{2}\right)^{v} + \left(\frac{l}{2} - l_{\mathrm{bd}}\right)^{v}} \tag{3.19}$$

here: $E_{\mathrm{c,cr}}$ is the concrete deformation modulus for a fully cracked element.

Incremental function Constant:

$$c = E_{\mathrm{c}} - a \cdot \left(\frac{l}{2} - l_{\mathrm{bd}}\right)^{v} \tag{3.20}$$

According to Equation 3.12, taking into account all the variables influencing the bond (shear) force between the concrete and the carbon fibre, the equation of the shear force in the crack influence zone is derived:

$$T_{\mathrm{lbd}}(x) = \left( \varepsilon_{\mathrm{slip,lbd}}(x) - \frac{M_{\mathrm{Ek}}(x)}{W_1 \cdot E_{\mathrm{c,lbd}}(x) \cdot \left(1 + \frac{1}{a_{lbd}(x)}\right)} - \frac{M_{\mathrm{Ek}}(x)}{W_2 \cdot E_{\mathrm{CFRP}} \cdot (1 + a_{lbd}(x))} \right) / \left( \frac{\frac{e_1}{a_{\mathrm{lbd}}(x)} - e_2}{W_1 \cdot E_{\mathrm{c,lbd}}(x) \cdot \left(1 + \frac{1}{a_{\mathrm{lbd}}(x)}\right)} - \frac{1}{A_{\mathrm{c}} \cdot E_{\mathrm{c,lbd}}(x)} - \frac{e_1}{W_1 \cdot E_{\mathrm{c,lbd}}(x)} + \frac{e_2 \cdot a_{\mathrm{lbd}}(x) - e_1}{W_2 \cdot E_{\mathrm{CFRP}} \cdot (1 + a_{\mathrm{lbd}}(x))} - \frac{1}{A_{\mathrm{CFRP}} \cdot E_{\mathrm{CFRP}}} - \frac{e_2}{W_2 \cdot E_{\mathrm{CFRP}}} \right) \tag{3.21}$$

The tangential bond stress in the crack zone is obtained by differentiating the contact (shear) force (3.21) along the axis of the element:

$$\tau_{\mathrm{lbd}}(x) = \frac{\partial T_{\mathrm{lbd}}(x)}{b_{\mathrm{CFRP}} \cdot \partial x} \tag{3.22}$$

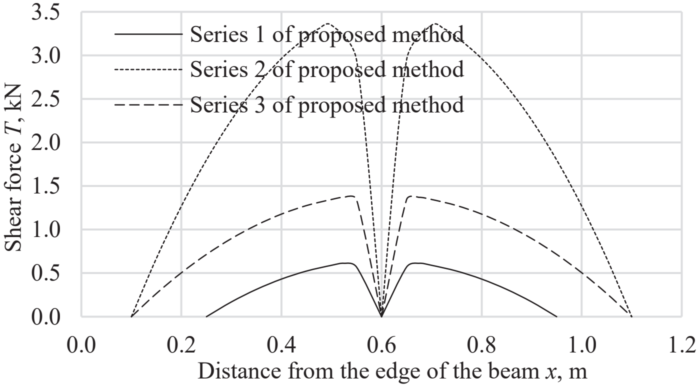


**Figure 11** Distribution of the shear force between carbon fibre and concrete over the length of the element by using the proposed method for series 1–3 composite beams

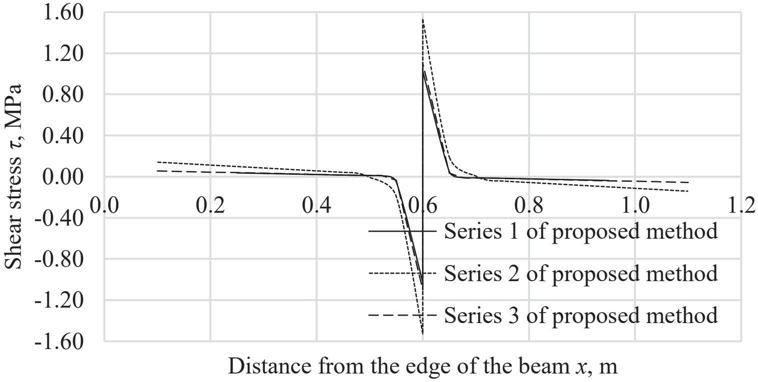


**Figure 12** Distribution of the shear stress between carbon fibre and concrete over the length of the element by using the proposed method for series 1–3 composite beams

According to the proposed analytical methodology, Figures 11 and 12 show the variation of the shear force and the tangential stress between the concrete and the carbon fibre over the length of the element when the crack is open in the mid-span of Series 1–3 composite beams. The contact shear force increases from the beam support to the crack influence zone, and, after reaching this zone, it starts to decrease rapidly until it reaches 0 kN at the crack. The reverse process is obtained with regard to the tangential stress which decreases from the beam support towards the mid-span of the beam to the crack zone of the influence, and, after reaching it, begins to grow rapidly and reaches its maximum at the crack. The contact shear stress in the mid-span of the beam is significantly higher than the stress at the carbon fibre ends. The difference ranges from 10.8 to

27.9 times, depending on the series. This increase of stress at the crack may reduce the bond of the carbon fibre to the reinforced concrete beam greatly.

## 4. NUMERICAL MODELLING OF FLEXURAL REINFORCED CONCRETE BEAMS STRENGTHENED WITH CARBON FIBRE

### 4.1. Formation of the finite element model

A finite element model was created for analysis and comparison of reinforced concrete beams strengthened with carbon fibre to the experimental results. The model was created by using the *Abaqus* finite element software. Quarter beam models were modelled to reduce the calculation resources. The finite element model, the finite element size and the elements are shown in Figure 13. The beam support of steel, the reinforced concrete beam and the load support were designed as 8-node linear bricks (C3D8R). As carbon fibre is extremely thin compared to the other elements, it was modelled as a 4-node doubly curved thin shell (S4R). Longitudinal and transverse reinforcement was modelled as a 2-node linear 3-D truss (T3D2). The size of the concrete cubes was 10 mm; carbon fibre – 16.6 mm; rebars – 20 mm.

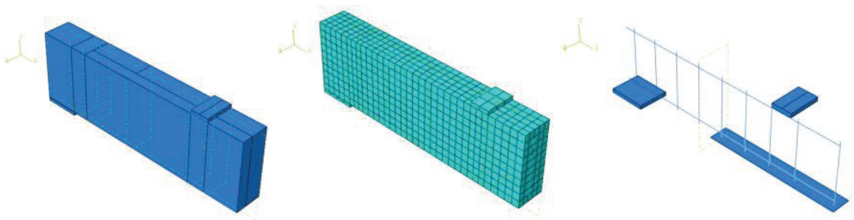

a) b) c)

**Figure 13** Images of a reinforced concrete beam strengthened with carbon fibre in *Abaqus*: (a) general view of the beam; (b) view of the finite elements of the beam; (c) view of all elements separately excluding concrete

The bond between the rebars and the concrete is assumed to be ideal. The bond between the carbon fibre and the concrete was described as a 'surface-to-surface' contact, interaction properties as 'normal behaviour, cohesive behaviour and damage'. The contact transfer was assumed as 'hard contact'. Table 4 shows the parameters of contact as used in *Abaqus* and as suggested by other authors (Arruda et al., 2016; Bsisu et al., 2017; Camata et al., 2015; Francois et al., 2002; Niu et al., 2006; Obaidat et al., 2010; Rizkalla et al., 2002; Saadatmanesh et al., 1998). After calculating the composite beam according to the extreme values of the contact stiffness parameters, it was found that the parameter values did not have a significant effect. The difference was up to 6.2%.

**Table 4** Parameters of contact in *Abaqus*

| Contact properties | Value accepted in FE model | Range of values from other authors |
|---|---|---|
| Normal stiffness, $K_{nn}$ MPa/mm | 2063 | 16.5–12800 |
| Shear stiffness, $K_{tt}$ MPa/mm | 2063 | 0.41–2900 |
| Max nominal (shear) stress MPa | 25 | 0.21–25 |
| Total/Plastic displacement $\delta_{pl}$ mm | 1.0 | 0.127–1.0 |
| Viscosity coefficient | 0.001 | 0.001 |

The displacement controlled load is applied to the beam so that to avoid potentially mathematically unsolvable equations in the calculation program.

**4.2. Results**

The numerical results obtained by using the finite element software *Abaqus* are presented and compared to the experimental results, standard *Euronorm* results and the iteration method results (Figure 14). Calculations were performed for Type A composite beams which did not have initial cracks. The maximum load limit of 100 kN was selected.

When summarizing the deflection calculation results of Type A beams according to various methodologies, it can be stated that the most similar results in terms of absolute values were obtained by using the finite element and the layer methods. The largest difference was 0.8 mm. In terms of absolute deflection values, the results differed most from the experimental results when comparing to the results obtained by using the formulas of EC2 (1.0 mm).

When comparing the similarity of the curve shape over the whole loading history, the most similar results were obtained by using the layer method for A1 beam, by using the formulas of EC2 and the finite element method for A2 beam, and by using EC2 formulas for A3 beam. The largest differences between the experimental results and the analytical or numerical calculation results were obtained when cracks were opening in the tensile zone and when the deflections were measured at the maximum load (100 kN). This may have been due to the fact that the selected calculation models of the tensile concrete materials calculate the strength of the tensile concrete inaccurately and take into account the elastic-plastic performance of the concrete. More significant differences, while obtaining smaller deflections according to the different calculation methodologies at the maximum measured load of 100 kN, can be obtained due to the slip between the concrete and the carbon fibre. The higher is the slip between the different materials, the higher deflections occur.

The calculation methodology of deflections adopted in EC2 for the calculation of the reinforced concrete beams estimating the influence of the cracks can also be applied to reinforced concrete beams strengthened with carbon fibre.

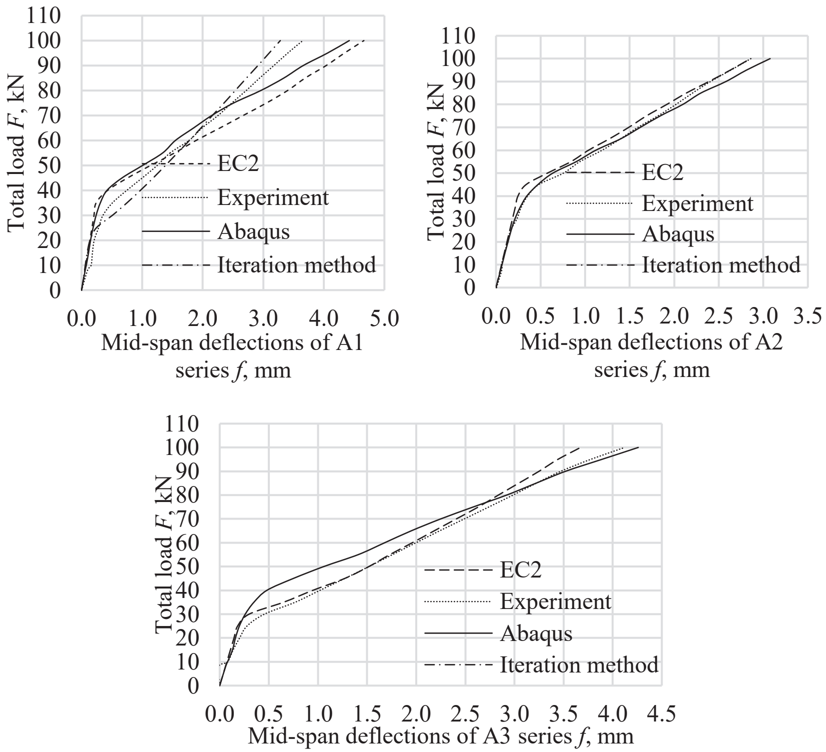


**Figure 14** Comparison of the total load-deflection curves according to the standart Euronorms, experimental results, the finite element method and the analytical iteration method: first diagram – A1 beam; second diagram – A2 beam; third diagram – A3 beam

## CONCLUSIONS

1. After the literature review, it was observed that the currently available research pays great attention to the anchorage of the carbon fibre of the composite beam. A common type of the cross-section failure is the loss of the carbon fibre bond to the concrete surface. However, no detailed analytical methodology has been created previously to estimate the pre-strengthening initial cracks of the beam, which affects the effective bond.
2. The load-bearing capacity of the beams strengthened with carbon fibre increased from 9.2% to 45% depending on the method of strengthening and the width of the initial cracks of the beam. The load-bearing capacity of the beams with the highest initial cracks width (the reinforcement has yielded) increased from 23% to 45%, while the beams without initial cracks increased from 9.2% to 27%. One of the possible reasons for the higher load-bearing

capacity of the damaged beams is the residual elastic-plastic strains of the rebars and concrete, which resulted in the higher stress in the rebars and lower stress in the carbon fibre compared to the undamaged beams at the same loads. Another reason is the lower deflection of the damaged composite beams after strengthening and the possible filling of the cracks with resin during the gluing of the fibres.

3. The proposed method is much easier than the theory of the built-up bars to apply in practice, as it is possible to take into account the different load distributions without solving complex differential equations. The proposed method can calculate the shear stress in the contact zone of the cracked element in the crack zone of influence which is significantly higher than the stress at the ends of the carbon fibre. The difference ranges from 10.8 to 27.9 times, depending on the type of the series. This increase in stress at the crack may greatly reduce the bond of the carbon fibre to the reinforced concrete beam.
4. For beam A3, the maximum value of shear stress calculated at the crack zone calculated by the proposed method is 27.3% lower than that obtained by the *Abaqus* program. It should be noted that the accuracy of the proposed method is greatly influenced by the length of the fibre anchorage, and, in the case of the *Abaqus* model, the chosen dimension of the mesh and the parameters describing the bond of concrete and fibre.
5. The standard deviation of the deflections of type A beams, calculated according to various methodologies, varies from 0.12 mm to 0.24 mm as the deviation is calculated from the average of all deflections, and from 0.16 mm to 0.29 mm, as the deviation is calculated from the experimental values. The coefficient of variation varies from 0.18 to 0.23 and from 0.20 to 0.26, respectively.

## REFERENCES


1. ALHASSAN, M. A., AL-ROUSAN, R. Z., and H. M., TAHA. Precise finite element modelling of the bond-slip contact behavior between CFRP composites and concrete. *Construction and Building Materials* [interactive]. 2020, *11*(240), 1–11. Elsevier Ltd. ISSN 0950-0618. Available at doi: 10.1016/j.conbuildmat.2019.117943
2. ARRUDA, M. R. T., FIRMO, J. P., CORREIA, J. R., and C. Tiago. Numerical modelling of the bond between concrete and CFRP laminates at elevated temperatures. *Engineering Structures* [interactive]. 2016, *110*, 233–243. Elsevier Ltd. ISSN 0141-0296. Available at doi: 10.1016/j.engstruct.2015.11.036
3. BALEVIČIUS, R., and M. Augonis. The effects of bond, shrinkage and creep on cracking resistance of steel and GFRP RC members. *Composite Structures* [interactive]. 2018, *187*(December 2017), 85–101.

4. BSISU, K. A., Hussein, H., and S. SARGAND. The Use of Hashin Damage Criteria, CFRP – Concrete Interface and Concrete Damage Plasticity Models in 3D Finite Element Modeling of Retrofitted Reinforced Concrete Beams with CFRP Sheets. *Civil engineering* [interactive]. 2017, *14*, 1171–1184.
5. CAMATA, G., SPACONE, E., AL-MAHAIDI, R., and V. Saouma. Analysis of Test Specimens for Cohesive Near-Bond Failure of Fiber-Reinforced Analysis of Test Specimens for Cohesive Near-Bond Failure of Fiber-Reinforced Polymer-Plated Concrete. *Journal of Composites for Construction* [interactive]. 2015, *10*, 528–538.
6. CHEN, C., SUI, L., XING, F., LI, D., ZHOU, Y., and P. LI. Predicting bond behavior of HB FRP strengthened concrete structures subjected to different confining effects. *Composite structure* [interactive]. 2018, *14*(187), 212–225.
7. Daugevičius, M. Influence of long-term load on the behaviour of reinforced concrete beams strengthened with carbon fibre composite. *Doctoral dissertation*. 2010.
8. DRIZORO. Repair and strengthening system based on carbon fiber sheets. *Technical bulletin8*.
9. ELGHAZY, M., REFAI, A. El, EBEAD, U., and A. Nanni. Experimental results and modelling of corrosion-damaged concrete beams strengthened with externally-bonded composites. *Engineering Structures* [interactive]. 2018, *172*, 172–186. Elsevier. ISSN 0141-0296. Available at doi: 10.1016/j.engstruct.2018.06.037
10. ESFAHANI, M. R., KIANOUSH, M. R., and A. R. TAJARI. Flexural behaviour of reinforced concrete beams strengthened by CFRP sheets. *Engineering Structures* [interactive]. 2007, *29*, 2428–2444.
11. *fib*. *Externally bonded FRP reinforcement for RC structures. Technical report bulletin 14*. 2001, 138.
12. FRANCOIS, B. B., DAVID, E., and E. RAGNEAU. Finite element modelling of flexural behaviour of externally bonded CFRP reinforced concrete structures. *Engineering Structures*. 2002, *24*(24), 1423–1429.
13. GUO, J. D. *Interfacial models for fiber reinforced polymer (FRP) sheets externally bonded to concrete*. Doctoral dissertation. 2003, *6*.
14. GUO, Z. G., CAO, S. Y., SUN, W. M., and X. Y. LIN. Experimental study on bond stress-slip behaviour between FRP sheets and concrete. *Proceedings of the International Symposium on Bond Behaviour of FRP in Structures*. 2005, *7*, 77–83.
15. LISAUSKAS, T., AUGONIS, M., and Š. KELPŠA. The Stress's State Analysis of Carbon Fibre Reinforced Concrete Elements Evaluating the Bond Influence. *Journal of Sustainable Architecture and Civil Engineering* [interactive]. 2018, *2*(23), 79–85.

16. LORENZIS, L. De, MILLER, B., and A. NANNI. Bond of FRP laminates to concrete. *ACI Materials Journal*. 2001, *28*(3), 256–264.
17. *LST EN 1992-1-1. Eurokodas 2. Gelžbetoninių konstrukcijų projektavimas. 1-1 dalis*. 2007, *234*. Vilnius.
18. *LST EN 12390-3:2009. Sukietėjusio betono bandymai. 3 dalis. Bandinių gniuždomasis stipris*. 2009. Vilnius.
19. *LST EN 12390-13:2013. Sukietėjusio betono bandymai. 13 dalis. Kirstinio tamprumo modulio nustatymas gniuždant*. 2013. Vilnius.
20. MOFRAD, M. H., MOSTOFINEJAD, D., and A. HOSSEINI. A generic non-linear bond-slip model for CFRP composites bonded to concrete substrate using EBR and EBROG techniques. *Composite Structures* [interactive]. 2019, *220*, 31–44.
21. MUKHTAR, F. M., and R. M. FAYSAL. A review of test methods for studying the FRP-concrete interfacial bond behavior. *Construction and Building Materials* [interactive]. 2018, *169*, 877–887. Elsevier Ltd. ISSN 0950-0618. Available at doi: 10.1016/j.conbuildmat.2018.02.163
22. NIU, H., and Z. WU. Effects of FRP-Concrete Interface Bond Properties on the Performance of RC Beams Strengthened in Flexure with Externally Bonded FRP Sheets. *Journal of Materials in Civil Engineering* [interactive]. 2006, *18*(October), 723–731.
23. OBAIDAT, Y. T., HEYDEN, S., and O. DAHLBLOM. The effect of CFRP and CFRP/concrete interface models when modelling retrofitted RC beams with FEM. *Composite Structures* [interactive]. 2010, *92*(6), 1391–1398. Elsevier Ltd. ISSN 0263-8223. Available at doi: 10.1016/j.compstruct.2009.11.008
24. RIZKALLA, S. H., BUSEL, J. P., BAKIS, C. E., BALAGURU, P. N., BALLINGER, C. A., BANK, L. C., BELARBI, A., et al. *Guide for the Design and Construction of Externally Bonded FRP Systems for Strengthening Concrete StructuresACI 440.2R-02*. 2002.
25. SAADATMANESH, H., and A. M. MALEK. Design Guidelines for Flexural Strengtheningof RC Beams with FRP Plates. *Journal of Composites for Construction*. 1998, *2*(4), 158–164.
26. WAN, B., JIANG, C., and Y. F. WU. Effect of defects in externally bonded FRP reinforced concrete Concrete substrate. *Construction and Building Materials* [interactive]. 2018, *172*, 63–76. Elsevier Ltd. ISSN 0950-0618. Available at doi: 10.1016/j.conbuildmat.2018.03.217
27. ZABULIONIS, D. Stress and strain analysis of a bilayer composite beam with interlayer slip under hygrothermal loads. *Mechanika*. 2005, *6*(56), 5–12.
28. ZADLAUSKAS, S. T*he research on cracking and deformation of reinforced concrete bridges under static and dynamic loads.* Doctoral dissertation. 2013.

29. РЖАНИЦЫН, А. Р. *Строительная механика*. Москва: Высшая школа, 1982.

## PUBLICATIONS ON THE SUBJECT OF THE DISSERTATION

### Publication in a journal indexed on the *Clarivate Analytics Web of Science* list

1. Lisauskas, T., Augonis, M., Zingaila, T., and M. R. T. Arruda. Stiffness and Strength Analysis of Flexural RC Beams Strengthened with CFRP Sheets Considering the Influence of Pre-cracking. *Mechanics = Mechanika*. Kaunas University of Technology. Kaunas: Technologija. ISSN: 1392-1207, eISSN: 2029-6983. 2020. Vol. 26, No. 4, p. 277–284. http://dx.doi.org/10.5755/j01.mech.26.4.25064

### Other publications in journals indexed in international databases

2. Lisauskas, T., Augonis, M., and Š. Kelpša. The Stress's State Analysis of Carbon Fibre Reinforced Concrete Elements Evaluating the Bond Influence. *Journal of Sustainable Architecture and Civil Engineering = Darnioji Architektūra ir Statyba.* Kaunas University of Technology. Kaunas: Technologija. ISSN: 2029-9990, eISSN: 2335-2000. 2018. Vol. 2. No. 23, p. 79–85. http://dx.doi.org/10.5755/j01.sace.23.2.20987

### Proceedings of international conferences

1. Lisauskas, T., Augonis, M. The Analysis of the State of Stress of Carbon Fiber reinforced Concrete Elements Evaluating the Influence of the Bond. *Advanced Construction 2018: Proceedings of 6th International Scientific Conference = Pažangioji Statyba 2018: 6-osios tarptautinės mokslinės konferencijos pranešimai.* Kaunas University of Technology. Kaunas: Technologija. ISSN: 2029-1213, eISSN: 2338-8983. 2018. p. 55–56. http://dx.doi.org/10.5755/e01.2538-8983.2018.

2. Lisauskas, T., Augonis, M. The Strength and Stiffness Analysis of Carbon fiber Reinforced Concrete Elements Evaluating the Influence of the Precracks. *13th International Conference „Modern Building Materials, Structures and Techniques" = 13-oji tarptautinė konferencija "Modernios Statybinės Medžiagos, Konstrukcijos, Metodai.* Vilnius Gediminas Technical University. Vilnius: Technika. 2019.

## Information about the author

Tadas Lisauskas was born on April 6, 1991 in Kaunas, Lithuania.
Email: tadaslisauskas@gmail.com.
1998-2010 Kaunas Simonas Daukantas secondary school.
2010-2014 Bachelor studies of Civil Engineering and BA (Honours) degree at Kaunas University of Technology, Faculty of Civil Engineering and Architecture.
2014-2016 m. Master studies of Construction and MA (Honours) degree at Kaunas University of Technology, Faculty of Civil Engineering and Architecture.
2016-2020 doctoral studies of Civil Engineering at Kaunas University of Technology, Faculty of Civil Engineering and Architecture.

## Scientific internships

Internship at the University of Žilina, Slovakia, from February 18 to March 15, 2019. Completed course: Reliability and reconstruction of engineering construction.

## Acknowledgments

The author of the doctoral dissertation expresses great gratitude to the scientific supervisor assoc. Prof. Dr. Mindaugas Augonis of the Faculty of Civil Engineering and Architecture, KTU, for all kinds of help and insights during the preparation of the doctoral dissertation.

The author also thanks scientific advisor Dr. Mário Rui Tiago Arruda of the Instituto Superior Técnico, University of Lisbon, Dr. Tadas Zingaila and doctoral student Deividas Martinavičius of the Faculty of Civil Engineering and Architecture, KTU, for the consultations about the finite element method. The author is also grateful to Dr. Šarūnas Kelpša for the advice and support while planning the experiment and Justinas Valeika for the consultations about translating the summary into English.

For the moral support and understanding, the author is grateful to his family, relatives and friends.

## REZIUMĖ

Daktaro disertacijoje analizuojami naujausi tyrimai apie gelžbetoninių konstrukcijų stiprinimą anglies plaušu bei kontakto zonos tarp anglies plaušo ir betono parametrus. Aprašyti analitiniai metodai galintys įvertinti kompozitinių sijų stiprumą, standumą ir galimą maksimalią sukibimo jėgą. Eksperimento metu nustatytos skirtingo stiprumo betonų mechaninės savybės ir armatūros stipris. Išmatuoti gelžbetoninių sijų įlinkiai apkrovimo metu ir plyšio pločiai po pradinio apkrovimo. Išmatuoti kompozitinių sijų suirimo jėga, įlinkiai bei betono ir anglies plaušo santykinės deformacijos. Remiantis atlikto eksperimento duomenimis buvo atlikti įlinkio skaičiavimai pagal EC2 metodiką. Gauti eksperimento rezultatai lyginami su iteracijų metodu, ACI, ISIS ir *fib* normomis. Buvo pasiūlytas analitinis modelis aprašantis kontakto jėgą ir įtempius tarp anglies plaušo ir betono. Gauti rezultatai lyginami su sudėtinių strypų teorijos gautais rezultatais. Buvo papildytas siūlomas analitinis metodas. Papildytas analitinis metodas gali aprašyti sukibimo jėgą ir šlyties įtempius supleišėjusiems (su mažu pleišėjimo intensyvumu) elementams per elemento ilgį, gauti rezultatai patikrinami baigtinių elementų metodu. Šis metodas yra lengvai pritaikomas praktikoje, nes galima įvertinti įvairius apkrovimo būdus išvengiant sudėtingų diferencialinių lygčių sprendimo. Baigtinių elementų metodu apskaičiuota gelžbetoninė sija sustiprinta anglies plaušu, analizuoti parametrai aprašantys sukibimą tarp anglies plaušo ir betono, gautos įlinkių kreivės nuo veikiamos apkrovos, kurios lyginamos su atliktu eksperimentu.

### Darbo uždaviniai

1. Atlikti lenkiamų gelžbetoninių sijų, sustiprintų anglies plaušu, naujausių tyrimų apžvalgą. Apžvelgti gelžbetoninių sijų stiprinimo būdus ir plaušo savybes. Išanalizuoti skaičiavimo metodus, aprašančius gelžbetoninių sijų, sustiprintų anglies plaušu, stiprumą ir standumą.
2. Atlikti lenkiamų gelžbetoninių sijų, sustiprintų anglies plaušu, pleišėtumo, standumo ir stiprumo eksperimentinius tyrimus. Išmatuoti parametrus, kurie padėtų nustatyti anglies plaušo praslydimą nuo betono.
3. Sudaryti analitinį modelį, kuriuo remiantis būtų galima įvertinti lenkiamo supleišėjusio (kai mažas pleišėjimo intensyvumas) kompozito sukibimo (šlyties) jėgą ir tangentinius (šlyties) įtempius tarp anglies plaušo ir betono, įvertinant sluoksnių praslydimą per elemento ilgį. Apskaičiuoti kompozito charakteristikas pagal kitų autorių siūlomas metodikas arba klasikinius skaičiavimo principus. Gautus rezultatus palyginti su eksperimentiniais rezultatais.
4. Atlikti lenkiamų gelžbetoninių sijų, sustiprintų anglies plaušu, skaičiavimus baigtinių elementų metodu.

**Tyrimų metodika**

1. Mokslinių publikacijų, knygų ir normų skaitymas, nagrinėjimas bei analizė.
2. Kompozitinės sijos bandomos universaliuoju presu. Plyšiai matuojami žiūroniniu matuokliu, plyšių liniuote ir mechaniniais (laikrodiniais) poslinkių matuokliais. Betono deformacijos matuojamos mechaniniais (laikrodiniais) poslinkių matuokliais. Kompozitinės sijos anglies plaušo ir betono tarpusavio praslydimas nustatomas matuojant deformacijas elektroniniais jutikliais. Įlinkiai matuojami linijiniais poslinkių matuokliais.
3. Skaičiavimas iteracijų metodu, sudėtinių strypų teorijos principu, ACI, ISIS, *fib*, EC2 ir kitais metodais.
4. Skaitiniai skaičiavimai baigtinių elementų programa „Abaqus“.

**Mokslinio darbo naujumas**

Sudarytas lenkiamo nesupleišėjusio ir supleišėjusio (kai mažas pleišėjimo intensyvumas) kompozito šlyties jėgos bei įtempių tarp anglies plaušo ir betono analitinis modelis, kurį taikant įvertinamas sluoksnių praslydimas per elemento ilgį ir apskaičiuojami plyšio zonoje ženkliai padidėję šlyties tarp anglies plaušo ir betono įtempiai, lemiantys greitesnį kontakto praradimą šioje zonoje.

Ištirta gelžbetoninių sijų pažaidų mastelio įtaka anglies plaušu sustiprintų sijų laikomajai galiai bei standumui ir nustatyta, kad labiausiai padidėja tų sijų laikomoji galia, kurių pradinių plyšių plotis buvo didžiausias.

**Darbo praktinė reikšmė**

Pasiūlytas analitinis skaičiavimo metodas lenkiamų supleišėjusių (kai mažas pleišėjimo intensyvumas) kompozitų sukibimo jėgai tarp dviejų sluoksnių nustatyti, įvertinant jų praslydimą. Analitiniu modeliu galima įvertinti sluoksnių sukibties standumą, esant įvairiems apkrovimo atvejams, šį modelį galima taikyti stiprinamų konstrukcijų projektavimui. Pasiūlytas metodas leidžia ne tik santykinai lengviau apskaičiuoti sukibimo įtempius ir šlyties jėgą tarp sluoksnių, išvengiant diferencialinių lygčių sprendimo, palyginti su sudėtinių strypų teorija, tačiau ir įvertinti reikšmingą plyšių įtaką. Taigi, siūlomam metodui, leidžiančiam įvertinti kompozito kontakto elgseną, kai atsiveria plyšys, būdingos platesnės pritaikymo galimybės.

**Ginamasis teiginys**

Anglies plaušu sustiprintų lenkiamų gelžbetoninių elementų šlyties įtempius, atsivėrus plyšiui tempiamoje betono zonoje, galima pakankamai tiksliai prognozuoti, įvertinus kintantį elemento skerspjūvio standumą plaušo inkaravimo zonoje ties plyšiu.

## IŠVADOS

1. Išanalizavus literatūrą, nustatyta, kad iki šiol atliktuose tyrimuose reikšmingas dėmesys skiriamas anglies plaušo inkaravimo užtikrinimui. Dažnai pasitaikantis kompozito suirimo pobūdis yra anglies plaušo sukibimo su betono paviršiumi praradimas, tačiau nėra pasiūlyto detalaus analitinio modelio, kuriuo būtų galima įvertinti sukibimą tarp anglies plaušo ir betono, kai gelžbetoninėje sijoje atsiveria plyšiai, paveikiantys tiek sijos stiprumą, tiek standumą.
2. Anglies plaušu sustiprintų sijų laikomoji galia padidėjo nuo 9,2 % iki 45 %, priklausomai nuo plaušo kiekio ir stiprinamų sijų supleišėjimo intensyvumo. Labiausiai padidėjo sijų su didžiausiais pradinių plyšių pločiais laikomoji galia (armatūrai pasiekus takumo ribą) – nuo 23 % iki 45 %, o mažiausiai – sijų be pradiniu plyšių – nuo 9,2 % iki 27 %. Viena priežasčių, kuri tai galėtų paaiškinti, yra liekamosios tampriai-plastinės armatūros ir betono deformacijos, dėl kurių didesni įtempiai pasiekti armatūroje ir mažesni – anglies plauše, palyginti su nepažeistomis sijomis. Kita priežastis – supleišėjusių sijų mažesnis įlinkis po sustiprinimo ir galimas plyšių užpylimas klijais plaušo klijavimo metu.
3. Siūlomas metodas gali būti plačiau taikomas praktikoje negu sudėtinių strypų teorijos metodas, kadangi juo galima įvertinti įvairius apkrovimo atvejus, išvengiant sudėtingų diferencialinių lygčių sprendimo. Siūlomu metodu galima apskaičiuoti supleišėjusios kompozitinės sijos kontakto šlyties įtempius, kurie plyšio veikimo zonoje yra gerokai didesni už įtempius anglies plaušo galuose. Šis skirtumas nagrinėtose sijose siekia nuo 10,8 iki 27,9 kartų, priklausomai nuo sijų tipo. Toks šlyties įtempių padidėjimas plyšio veikimo zonoje sumažina anglies plaušo sukibimą su gelžbetonine sija.
4. A3 sijai plyšio vietoje didžiausia šlyties įtempių reikšmė, apskaičiuota siūlomu metodu, gauta 27,3 % mažesnė nei gauta programa „Abaqus“. Pažymėtina, kad siūlomo metodo tikslumui reikšmingos įtakos turi plaušo inkaravimo ilgis, o „Abaqus“ modelio – pasirinktas elementų tinklelio matmuo bei betono ir plaušo sukibimą apibūdinantys parametrai.
5. A tipo sijų įlinkių, apskaičiuotų pagal įvairias metodikas, standartinis nuokrypis kinta nuo 0,12 mm iki 0,24 mm kaip nuokrypis, apskaičiuotas nuo visų įlinkių vidurkio, bei nuo 0,16 mm iki 0,29 mm kaip nuokrypis, apskaičiuotas nuo eksperimentinių reikšmių. Variacijos koeficientas atitinkamai kinta nuo 0,18 iki 0,23 ir nuo 0,20 iki 0,26.

**Informacija apie autorių**

Tadas Lisauskas gimė 1991 m. balandžio 6 d. Kaune.
El. paštas: tadaslisauskas@gmail.com.
1998-2010 m. Kauno „Simono Daukanto“ vidurinė mokykla.
2010-2014 m. Statybos inžinerijos bakalauro studijos ir kvalifikacinis laipsnis su pagyrimu, Kauno technologijos universiteto Statybos ir architektūros fakultetas.
2014-2016 m. Statybos magistro studijos ir kvalifikacinis laipsnis su pagyrimu, Kauno technologijos universiteto Statybos ir architektūros fakultetas.
2016-2020 m. Statybos inžinerijos doktorantūros studijos, Kauno technologijos universiteto Statybos ir architektūros fakultetas.

**Mokslinės stažuotės**

2019 m. vasario 18 d. – kovo 15 d. – mokslinė stažuotė Žilinos universitete. Išklausytas modulis – inžinerinių konstrukcijų patikimumas ir rekonstrukcija.

**Padėka**

Autorius dėkoja moksliniam vadovui – Kauno technologijos universiteto Statybos ir architektūros fakulteto docentui dr. Mindaugui Augoniui už visokeriopą pagalbą ir įžvalgas rengiant daktaro disertaciją.

Už konsultacijas, skaičiuojant baigtinių elementų metodu, autorius dėkingas moksliniam konsultantui dr. Mario Rui Tiago Arruda, dr. Tadui Zingailai ir doktorantui Deividui Martinavičiui. Autorius taip pat dėkingas dr. Šarūnui Kelpšai už patarimus ir palaikymą planuojant eksperimentą bei Justinui Valeikai už konsultacijas verčiant tekstą į anglų kalbą.

Už moralinį palaikymą ir supratingumą autorius dėkingas savo šeimai, artimiesiems ir draugams.

UDK 624.072.2 + 624.012.45]043.3)

SL344. 2021-03-15, 2,25 leidyb. apsk. l. Tiražas 50 egz. Užsakymas 72.
Išleido Kauno technologijos universitetas, K. Donelaičio g. 73, 44249 Kaunas
Spausdino leidyklos „Technologija“ spaustuvė, Studentų g. 54, 51424 Kaunas